

# Investigation of Electro-optical Characteristic and Structure Optimization of PMMA: Bepq2/BCP/Tpbi Blue Highly Efficient OLED Device

Renu Sharma<sup>1\*</sup>, Ravi K. Maddila<sup>2</sup>

## Abstract

*In this Investigation, the energy level structure of the Spiro-MeOTAD/PMMA: Bepq2/BCP/Tpbi/LiF OLED has been investigated to explain the method of electron-hole charge carrier pair recombination and the light generation. The Maxwell-Boltzmann statistics model was applied to optimize the structure to reduce the band gap between conductive layers. We found the simulated results J-V, J-Illumination flux, and Current Efficiency (CE) characteristics when we applied forward bias. Inconclusive results determined the threshold voltage is 3.37 V. In addition, we study the impact of the variation in thickness of the Exciton/Electron blocking layer ( $x=500\text{\AA}$ ,  $600\text{\AA}$ ,  $900\text{\AA}$ ,  $1200\text{\AA}$ ) as BCP the behaviours of the electric and optical characteristics of the device and low  $CIE_y$  may satisfy the needs of a broad range of blue OLED with the emission of exciton of 450 nm. The CIE coordinates remain stable at (0.150,0.150) and PMMA: Bepq2 polymer layer can cover the blue area entirely. Additionally, we analysed the internal device physics mathematical model in terms of current density, hole-electron mobility, effective carrier concentration and recombination. Our study aims to pave the way for future research into the electro-optical effects of highly efficient and high-brightness blue OLED technology.*

**Keywords:** Illumination flux, Current efficiency, HOMO-LUMO energy levels, PMMA: Bepq2, BCP.

## INTRODUCTION

OLEDs are becoming popular for flexible thin-panel displays and solid-state lighting because of

### \*Author for Correspondence

Renu Sharma  
E-mail: 2019rec9001@mmit.ac.in

<sup>1</sup>Ph.D Research Scholar, Department of ECE (Electronics and Communication Engineering), Malaviya National Institute of Technology Jaipur, Jawahar Lal Nehru Marg, Jaipur, Rajasthan, India

<sup>2</sup>Assistant Professor, Department of ECE, Malaviya National Institute of Technology Jaipur, Jawahar Lal Nehru Marg, Jaipur, Rajasthan, India

Received Date: May 05, 2023

Accepted Date: May 17, 2023

Published Date: June 26, 2023

**Citation:** Renu Sharma, Ravi K. Maddila. Investigation of Electro-optical Characteristic and Structure Optimization of PMMA: Bepq2/BCP/Tpbi Blue Highly Efficient OLED Device. Journal of Polymer & Composites. 2023; 11(Special Issue 5): S56-S68.

benefits such as low weight, self-luminous nature, and complete colour range [1]. RGB light must be produced perfectly to provide full-colour display [2, 3]. Many researchers and investigators have primarily focused on four strategies to overcome blue OLED limitations for Blue OLEDs' poor efficiency: we invented deep-blue OLEDs with an EQE max of 6.65% and a y-axis of 0.058 in the ( $CIE_y$ ) [4].

Additionally, investigators have combined iridium metal and deep-blue phosphorescent OLEDs with luminescence maxima between 430 and 460 nm were conducted; the resulting EQEs ranged from 15 to 30 percent [5, 6]. Li et al. invented a cobalt-blue OLED with an EQE

maximum of 10.5% and a (CIE<sub>y</sub>) of 0.065 by pyrene [7]. In general, blue luminous materials' essential wide bandgap often outputs an imbalance charge carrier between carrier injection and transport, which raises the operating voltage and decreases device stability and efficiency [8, 9]. In 2020, Kazlauskas et al. investigated to able to produce blue (EL) with an EQE max of 17.0% (max 460 nm) [10]. However, it was still limited by an 18-hour device lifespan (95% of the original brightness). According to the findings, developing blue OLEDs concurrently have a long lifespan, [11, 12]. Here, we have read to satisfy the conditions mentioned above (DITBDAP). which was twice as long as the Bmpac based OLED (time to 95% of the starting brightness of 3000 (cd/m<sup>2</sup>)). At high brightness, the efficiency roll-off was very low, displaying 1% at 1100 cd/m<sup>2</sup> and 5% at 3200 cd/m<sup>2</sup> [13].

The spreading research of Blue OLEDs, the proposed OLED structure having Spiro MeOTAD as the hole Transport layer, PMMA: Bepq2 as the emissive layer, BCP as the Exciton/electron blocking layer and TpbI as electron transport layer, required calculations regarding the optical and electrical characteristics Max. Illumination flux, CE, Max. EQE and low CIE<sub>y</sub> may satisfy the needs of a broad range of blue OLEDs, and the CIE of PMMA: Bepq2 polymer layer can cover the blue area entirely [14]. Due to behaviour of charge density under biasing, in general blue luminous materials' intrinsic wide bandgap frequently leads to an imbalance carrier between the injection and transport layer, which elevates the operating voltage and reduces device stability and efficiency. So that we reduce this issue by using Maxwell-Boltzmann statistics for reducing bandgap between conductive layers, and we found that Max. Illumination flux, Max. CE and low CIE<sub>y</sub> may satisfy the needs of a broad range of blue OLED, and the CIE of PMMA: Bepq2 polymer layer can entirely cover the blue area.

### PROPOSED BLUE OLED DEVICE STRUCTURES AND SIMULATION PARAMETERS

High efficiency is critical for creating Blue OLED with low power consumption. Carrier injection, charge mobility, and device architecture are some variables affecting efficiency and other performance. For high-efficiency Blue OLED, a multi-layered device architecture that consists of specification thickness as follows:

Device: ITO (800Å)/Spiro-MeOTAD(500Å)  
 /PMMA: Bepq2(200Å)/BCP((x=500Å,600Å,900Å,1200Å)  
 /TpbI(200Å)/LiF (5Å)/Al (500 Å)

A multi-layered device architecture that consists of Spiro-MeOTAD is used as a hole transport layer. It has been increased for energy efficiency. Spiro-MeOTAD molecules show a low electrical conductivity. It has slower hole mobility desired to balance charge recombination as holes travel faster than electrons in organic materials; PMMA: Bepq2 as polymer nanocomposites revealed good transparency properties, thermal stability, and high electrical conductivity, making suitable materials as an emission layer as an emitting layer. The chemical structure is shown in Figure 1 [15]. And it also has excellent optical properties, with a refractive index of 1.490. With hosting material Bepq2 acts as an EML layer because Bepq2, a blue fluorescence emitter, has a unique charge transport ability. And Bathocuproine BCP(x=500°A,600°A,900°A,1200°A) is used as a blocking barrier because it has a high electron affinity.

TpbI, as the ETL is an electron transport layer, can not only block hole leakage from the EML but also have good electron transport properties. Besides, the effects of ETL to increase the efficiency of OLED are presented, and LiF (Lithium Fluoride) buffer layer interface the practical cathode work function to 4.3 eV can be reduced by pulling down the vacuum level. This layer also serves as a buffer, preserving the cathode's low work function and shielding the active layer from hot Al atoms during evaporation.

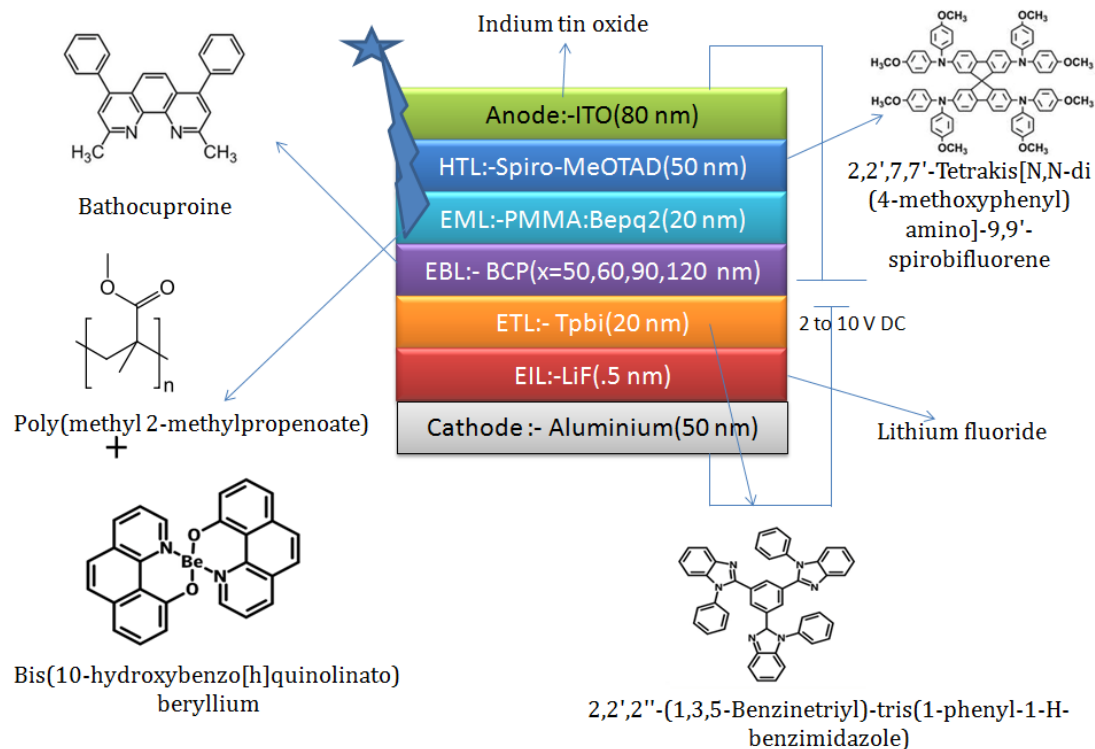


**Figure 1.** Proposed PMMA: Bepq2/BCP/Tpbi Blue OLED Device Structure.

Efficiency employed in the OLED structure between ITO as the p-type electrode is holed supplying a layer of OLED; the anode has a high work function so that the injection barrier between the adjacent organic layers and this anode layer should be reduced then effectively hole injected to the emission layer and gives maximum transparency (90%) to meditative light, maximum conductivity. And Al for n type electrode depends on the type of OLED required here and can be used transparent cathode. The interface of the electron transport layer, a basic design, and the emission layer are where this recombination should occur in theory. However, the organic materials employed in OLED devices have greater hole mobility than electron mobility. Due to this characteristic, the holes get to the cathode before the electrons do, and during this transition, the holes lose a large amount of energy. Carrier extinguishing is the term used for this. The OLED's emission efficiency is dramatically reduced due to carrier extinguishing. Due to solve this issue, several layers are employed to balance charge injection. The many layers are used for this purpose in all proposed OLED structures. The studied OLED device architecture is shown in Figure 1, together with the associated energy levels at threshold voltage 3.37 V. The molecular structures of the materials employed are shown in Figure 1.

### MATHEMATICAL ANALYSIS MODELING OF THE DEVICE WITH MAXIMUM EFFICIENCY AND SIMULATION PARAMETERS.

Here we have exposed the Mathematical Analysis modelling of the proposed Device and Simulation Parameters. Charge transport must be adequate to produce high-performance OLED devices. A thorough knowledge of the charge transport characteristics is necessary to advance toward more effective devices in this electronics area. The charge carrier mobility, a crucial charge transport parameter, measures how well a charge carrier will react to an applied electric field ( $F$ ), resulting from a potential between the contacts [16].

$$v_d = \mu F \quad (1)$$

where  $v_d$  represents the charge carriers' drift velocity. Charge transport will be diffusive in the absence of external fields, and a charge-mean-square carrier's displacement will be determined by

$$\langle x^2 \rangle = nDt \quad (2)$$

where  $D$  is the Einstein diffusion coefficient,  $t$  is time, and  $n$  is an integer corresponding to the system's dimension (for a 3D system,  $n = 6$ ) [16]. The mobility [16],

$$\mu = \frac{qD}{kBT} \quad (3)$$

where  $kBT$  is the thermal energy, determines how much a charge carrier may diffuse in a material [16]. We have designed model equations; a charge carrier's naturally random motion will acquire a little net velocity in the direction of the applied field when an electric field is used to it. The drift current is the current produced by an applied electric field. Here To represent the main attributes of charge carriers transport in OLED,

Using here Poisson's equation [17],

$$\nabla \cdot (\epsilon \nabla \psi) = q(n + n_{re} - p - p_{re}) \quad (4)$$

$$\rho = q(n + n_{re} - p - p_{re} + N_{acc} - N_{don}) \quad (5)$$

$$\nabla \cdot (\epsilon \nabla \psi) = \rho \quad (6)$$

where the device is assumed to be doping free ( $N_{acc} = N_{don} = 0$ ). The electrical potential drop  $\psi$  depends on the moving charge carrier's densities  $n$  and  $p$ , and the recombined charge carrier's densities  $n_{re}$  and  $p_{re}$  and  $q$  is the charge. Here is how an electron and hole eventually collide inside the emission layer to create the confined excited state known as excitons (photons). The polymer band gap  $E_g$  determines how long of a wavelength is emitted. And hence, you have the emission of a desired wavelength, so we can see the light wavelength of the light emission is related to, in the OLED, is equal to the energy difference means the band gap between the LUMO and HOMO of the organic material. Some energy corresponding to the difference is given up in heat and light. During recombination and the energy corresponding to the forbidden energy gap  $E_g$  is released. Hence electromagnetic waves are emitted.

$$E_g = h\nu \quad (7)$$

$$\nu = \frac{c}{\lambda} \quad (8)$$

put the value of  $\nu$

$$E_g = h \frac{c}{\lambda} \quad (9)$$

$$\lambda E_g = h \frac{c}{E_g} \quad (10)$$

Where  $h$  Planck's constant and  $c$  is the velocity of light, this shows that  $E_g \propto \frac{1}{\lambda}$ .

Poisson's equation and the current density drift-diffusion equations are included in OLED structure [18]. Poisson's equation relates the electron-holes (charge carrier) densities and the electrostatic potential. Gauss's Law:

$$\frac{d}{dx} \epsilon_0 \epsilon_r \frac{d\psi}{dx} = q(n - p). \quad (11)$$

where  $\epsilon_0$  the product of vacuum permittivity [18] and the relative permittivity  $\epsilon_r$  of the organic material. To simulate OLEDs by solving the Poisson equation [18], the bipolar drift diffusion equations and the carrier continuity in the time and 1D domains [17].

$$\frac{d}{dx} \epsilon_0 \epsilon_r \frac{d\psi}{dx} = q(p + p_t + p_d - n - n - n_d). \quad (12)$$

$$\frac{\partial p}{\partial t} = -\frac{1}{q} \frac{dJ_p}{dx} - R_L - R_{p,d}. \quad (13)$$

$$\frac{\partial n}{\partial t} = -\frac{1}{q} \frac{dJ_n}{dx} - R_L - R_{p,d} \quad (14)$$

The densities of recombined holes and electrons in the dopant layer are denoted by  $p_d$  and  $n_d$ , respectively. The current densities of free holes and electrons charge carriers are denoted by  $J_p$  and  $J_n$ , respectively.

Recombination coefficients are for free charge carriers, positive charge carriers, and meshed negative charge carriers in the dopant, and free negative charge carriers and meshed positive charge carriers in the dopant [17, 19].

$$r_L = \frac{q}{\epsilon_0 \epsilon_r} (\mu_n + \mu_p) \quad (15)$$

$$r_{p,d} = \frac{q}{\epsilon_0 \epsilon_r} \mu_p \quad (16)$$

$$r_{p,d} = \frac{q}{\epsilon_0 \epsilon_r} \mu_n \quad (17)$$

where the electron and hole mobilities, respectively, are  $\mu_n$  and  $\mu_p$  [19]. These equations can be used to characterize the density of holes and electrons by applying the Maxwell-Boltzmann statistics theory:

$$p = N_{HOMO} e^{\left(\frac{E_{HOMO} - E_{Fp}}{kT}\right)} \quad (18)$$

$$n = P_{LUMO} e^{\left(\frac{E_{Fn} - E_{LUMO}}{kT}\right)} \quad (19)$$

Where, respectively,  $k$  and  $T$  stand for the Boltzmann's constant and the device temperature; Charge carriers' respective quasi-Fermi levels are  $E_{Fn}$  and  $E_{Fp}$ ;  $N_{HOMO}$  and  $P_{LUMO}$  are the densities of energy levels respectively.

The following is a formula for the energy states of HOMO and LUMO [19]:

$$E_{HOMO} = -(q\psi + \chi_c + E_g) \quad (20)$$

$$E_{LUMO} = -(q\psi + \chi_c) \quad (21)$$

$\chi_c$  and  $E_g$  stand for the organic material's electron affinity and energy gap, respectively. Table 1 shows that the energy states of HOMO and LUMO in eV have given the proposed device different types of organic material layers.

### Calculation and Modelling of External Quantum Efficiency

Figure 2 roughly illustrates a typical multi-layered OLED structure used to  $\eta_{max}^o$  between a cathode with ambient and an anode with the substrate; the design contains  $m$  layers. The refractive indices and thickness of the materials in each layer  $j$  is represented by the variables  $n_j$  and  $d_j$ , respectively.

**Table 1.** The simulation parameters of materials for proposed OLED device

S.N.	Parameters /Materials	Spiro-MeOTAD (50 nm)	PMMA: Bepq2 (20 nm)	BCP (x=50 nm,60 nm,90 nm,120 nm)	Tpbi (20 nm)
1.	Electron mobility ( $m^{-2}v^{-1}s^{-1}$ )	1.0e-6	1.0e-6	1.0e-6	1.0e-6
2.	Hole mobility ( $m^{-2}v^{-1}s^{-1}$ )	.1	.01	.01	1.0e-6
3.	Effective density of free electron states ( $m^{-3}$ )	5.0e25	5.0e25	5.0e25	5.0e25
4.	Effective density of free hole states ( $m^{-3}$ )	5.0e25	5.0e25	5.0e25	5.0e25
5.	Temperature (K)	300	300	300	300
6.	LUMO level (eV)	2.6	2.7	2.8	2.7
7.	HOMO level(eV)	5.9	6.2	6.4	6.2
8.	Energy Bandgap(eV)	3.3	3.5	3.6	3.5
9.	Relative Permittivity (a. u.)	3.0	5.0	3.0	5.0

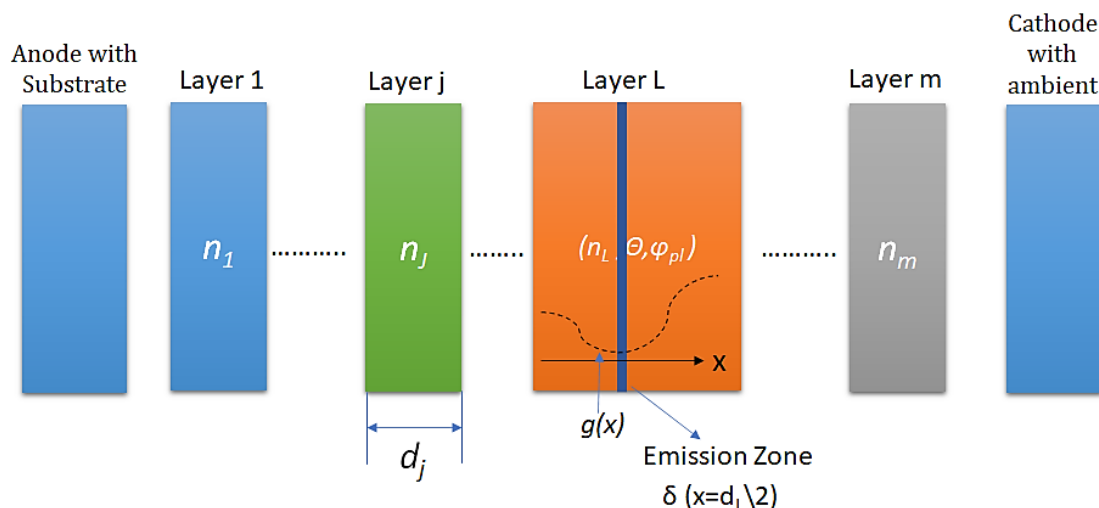


**Figure 2.** A multi-layered OLED structure used for the modelling of External Quantum Efficiency.

The EML of the device is placed at layer L, and the position of the emission zone adjusts a  $\delta$ ,  $\delta(x = \frac{dL}{2})$  [20]. It can also be expressed by the multiply between  $\eta_{int}^o$  and  $\eta_{out}^o$  [20].

$$\eta_{max}^o = \eta_{int}^o * \eta_{out}^o \quad (22)$$

Here,

$$\eta_{int}^o = \lambda_b * \eta_{s/t}^o * \eta_{pL}^o \quad (23)$$

then [20],

$$\eta_{max}^o = \lambda_b * \eta_{s/t}^o * \eta_{pL}^o * \eta_{out}^o \quad (24)$$

$\eta_{int}^o$  is calculated by the charge balance factor ( $\lambda_b$ , a fraction of radiative exciton ( $\eta_{s/t}^o$ ) [20], 0.25 for typical fluorescent emitters) and  $\eta_{pL}^o$  quantum yield OLED device efficiency.

$$\eta_{max}^o = \eta_{s/t}^o \cdot \max \left[ \int s(\lambda) \cdot \eta_{pL}^o(\Theta, \Gamma, \lambda) \cdot \eta_{out}^o(\Theta, \Gamma, \lambda) \cdot d\lambda \right] \quad (25)$$

The  $\Theta$ , the horizontal portion of the emitting dipoles,  $\Theta$  of the OLED structure has an impact on the Purcell effect, the out-coupling efficiency of the emitted light,  $\eta_{out}^o$ , which  $\eta_{pL}^o$  depends on the quantum yield in free space, the emitting dipole orientation factor, and the location of the emission zone in the device.

Where each layer's thickness is represented by  $\Gamma$  ( $d_1, \dots, d_m$ ), and the normalized photon spectrum of the emitter in free space is represented by  $s(\lambda)$  as a function of wavelength.

$$\eta_{pL}^o = \frac{G(\Theta, \Gamma, \lambda) \cdot \phi_{pL}}{1 - \phi_{pL} + G(\Theta, \Gamma, \lambda) \cdot \phi_{pL}} \quad (26)$$

In the structure [20],  $G$  is the Purcell factor which is the spontaneous emission rate. Here, the refractive indices of the layers, the PMMA: Bepq2's emitting dipole orientation ( $\Theta$ ). Now, if this OLED emits light, the amount that matters to us is the light output divided by the electric power; hence, if we are now interested in the OLED's efficiency, we should know that it relies on a variety of processes. If I use the unit of lumen per watt here and define OLED efficiency as the total light output divided by electric power, it would initially rely on the first step, the injection of carriers. The exciton, which emitted the light, was then produced by the carriers moving together electrons and holes. Hence, the effectiveness of that process will determine whether an exciton is made and, if so, the ratio of singlet to triplet. We will first determine how much of that exciton will emit light. Then the

quantum efficiency of an exciton will decide if the light is emitted as emission or non-emission radiation, as a radiative or non-radiative emission. Now, let us look at the  $\lambda$  term, which describes the device's charge balance factor. The first step in the process is the injection of carriers, which involves injecting carriers from the anode and cathode. However, for effective injection, an ohmic contact is required.

When the difference between the HOMO and the work function of the anode is high, and the LUMO and the work function of the metal are minimal, the contact will be ohmic. Because of this need, the barrier to carrier injection, which we refer to as the barrier to injection, must be minimal. Next, this electron must travel. It must go in the direction of the anode while the hole moves toward the cathode. It is an exciton creation, and as a result, the electron and hole's mobility in how they travel relative to one another and where they join. Hence, carriers' mobility, including electron and hole mobility in the organic layer, is the second crucial factor in charge balancing. Because the goal is for each electron injected from the Al into the PMMA: Bepq2 to create an exciton with each hole injected from the ITO, therefore, to achieve 100% efficiency, we must ensure that no electron passes from the Al to the ITO without first forming an exciton. It means that if we have 10 electrons injected from the Al and ten holes injected from the ITO, they must all recombine to create an exciton before emitting light. Our charge balance should be correct to get excellent charge and exciton generation. Since  $\mu_p$  mobility in organic materials is often significantly higher than  $\mu_n$  mobility, there is an issue here. Hence, plotting the recombination rate in this specific device reveals that all material recombines near the cathode. Because holes travel considerably more quickly than electrons, they all join near the cathode, which is problematic since this causes the excitons to be quenched.

Excitons result from being close to the cathode; hence it is necessary for this specific device that the mobilities of the two carriers also line up. Hence, what are the methods by which we can accomplish that? We may introduce, in addition to the device that we have discussed, which we had on the substrate, to do that. We started with ITO as the bottom electrode, and when I wanted to increase injection, I often put another layer on top of it. This layer increases injection, lowering the barrier brought on by the difference between the work function and LUMO level. Hence, this is referred to as the hole injection layer, and I also have the option of adding a layer on top of it called the hole transporting layer. Next, I have my organic emission substance; at this point, I'll use a few abbreviations. To assist the holes being injected from the anode side, I can do the same thing to the cathode side, which means adding an electron transport layer. Therefore, this would be the hole injection layer HIL, hole transporting layer HTL, and organic emission material.

To optimize this charge balance, a single-layer device that we just discussed may be transformed into a highly complicated multi-layer structure with the addition of an electron injection layer and a cathode. And the objective is to ensure that as much of the light created here is gathered outside as feasible. Another thing is that I may put another layer here, which we refer to as the charge carrier blocking layer, if these carriers move from the anode to the cathode at a much faster pace. To prevent the holes from moving toward the cathode, which improves the device's charge balance.

## RESULTS AND DISCUSSION

The primary goal was to implement blue OLEDs, which have a higher frequency and shorter wavelength and carry more energy than green and red light—utilizing a novel proposed OLED device structure and increasing their illumination flux with EQE. The performance of Spiro-MeOTAD/PMMA: Bepq2/BCP/Tpbi/LiF OLED device structure with a variation of thickness of the BCP layer is examined through electrical and optical analysis. They used the (OghmaNano) Organic and hybrid Material Nano Simulation tool. Simulator, the electro-optics characteristics of OLED are simulated. Where the three variables are current (I), voltage (V), and brightness ( $\text{cd/m}^2$ ). This  $(\text{cd/m}^2)/(\text{J})$  is a formula for calculating current efficiency. For power efficiency calculations “cd”

should be converted to "lumen". The lumen is a general measurement that measures perceived radiant light energy instead of actual radiant energy (all the EM energy). By the eye's reaction, it is a weighted unit. Maximum practical,  $\eta_0$  max, is determined by the ratio of the number of excitons radiated from the OLED's surface to the no. of electrons inserted. Numerous factors affect how well OLEDs perform. Remember that even a single restriction might make a gadget less effective. Chemistry-wise, the efficiency of a material is governed by its thermal, morphological, and electrochemical stability in addition to its quantum yield. For successful recombination of electrons and holes in the emission layer, we also need to match the energy levels of emission material with other layers (HTL, HBL, ETL, EBL, etc.) to lower the driving voltage and regulate the thickness of these layers. Even the method employed to deposit these layers (solvent process or vacuum deposition) considerably influences the efficiency. Investigated are the electrical and optical effects of applying an OLED voltage between 0.0 V and 3.5 V. If we can see that the OLED device has indium tin oxide as an anode, it has a work function concerning the vacuum level 4.7 electron volts. You know there is some vacuum level; we are showing these energies. And for the organic and LUMO come at HOMO is at 5.9 eV, and the lowest occupied one is around 2.8 eV for the cathode,

So, when we apply the forward bias to this device, electrons will be inserted into the PMMA: Bepq2, and on this side, holes will be inserted into the PMMA: Bepq2. This electron and holes will recombine to produce light, so the electron will recombine with the hole to produce light in this case. And hence, you have the emission of a desired wavelength, so we can see the light wavelength of the light emission is related to, in the OLED, is equal to the HOMO, the energy difference between the LUMO and HOMO of the organic material. We had the ITO as an electrode. If we want to improve the injection, we will add another layer, which enhances injection and improves this barrier caused by the difference in the work function and the HOMO level. So, this is known as the hole injection layer. The Spiro-MeOTAD layer now helps inject holes from the anode side; I can do the same to the cathode side, which means I can add a Tpb as the electron transport layer. And on that, I will add an electron injection layer and, finally, the cathode. A single-layer device, which we just discussed, can become a complex, multi-layered structure to improve this charge balance. And the goal here is to ensure that whatever light is generated here is collected outside the substrate as much as possible.

### Effect of Variation of BCP Thickness

In this paper, we have explained how to select many criteria parameters for the thicknesses of layers of the OLED device, like the value of HOMO and LUMO level, band gap, refractive index, mobilities of charge carriers, and minimum injection barriers between layers.

To maximize EL efficiency, the mobilities of charge carriers must be balanced. Adjusting the hole-blocking layer's thickness is accomplished. The hole-blocking layer offers a preferred channel for electrons to flow from the cathode to the emission layer and prevents holes from leaking toward the cathode (braking effect). We can balance the mobility of charge carriers in this manner. However, the emission layer might then become too concentrated with holes consequently.

We kept the thickness of all layer's constant, with the variation of the BCP layer, which was altered between 50 nm and 120 nm, to evaluate the effect of BCP thickness variation on brightness. We found that when BCP layer thickness increased from 50 nm to 60 nm, an applied voltage's brightness also increased. Yet, for the same applied voltage, the values of the illumination flux value fall when the thickness is raised above 90 nm. At the area where the thickness of the BCP layer is more than 60 nm, the applied voltage must be presented with the rise in BCP layer thickness to achieve a given brightness. The best illumination output based on a 50 nm thick BCP layer, while a 120 nm thick BCP layer represents the worst illumination output; this observation suggests that in the BCP layer's thickness, mainly when such changes occur when the layer's thickness exceeds 60 nm. The energy levels of our OLED's different layers are shown in Figure 3.

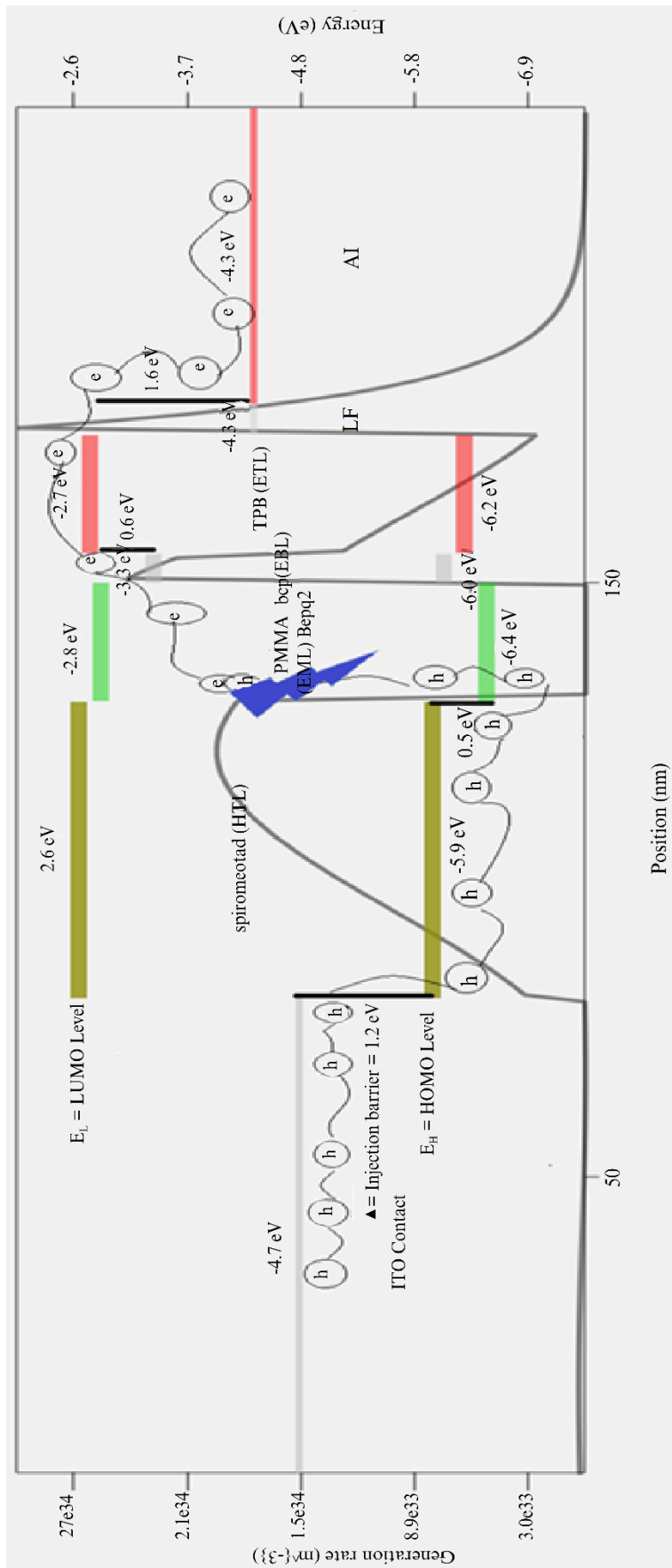


**Figure 3.** Energy levels of our OLED's different layers with effect of variation of BCP thickness.

Their energies at the interface between the BCP and PMMA: Bepq2 layer are near HOMO. The BCP layer presents a significant energy barrier (0.5 eV) that makes it challenging for holes to enter the cathode. As the BCP layer offers a preferred channel for electron transit, its thickness is a critical factor in controlling how holes and electrons are distributed about one another inside the emission layer. The property of the BCP layer to impose varying degrees of resistance to the flow of electrons and holes through it makes it work as a control value in terms of the flow of electrons and holes.

We may enhance the concentration of electrons and holes inside the emission layer by precisely adjusting the thickness of the BCP layer, which would lead to increased brightness from their radiative recombination in PMMA: Bepq2. Suppose the BCP layer's thickness kept rising (beyond 90 nm). In that case, the recombination zone will move from the PMMA: Bepq2 layer to the BCP layer, where excitons will be more likely to experience non-radiative decay close to the cathode and have a lower luminous efficiency consequently.

We changed the BCP layer's thickness from 50 nm to 60 nm in our investigation. Brightest brightness is attained when BCP thickness is optimized (50 nm), at which point the concentration of excitons generated in the PMMA: Bepq2 area is at its highest. We found Max. Current efficiency is 86.5 cd/A with Max. Illumination flux is 1071956.768(lumens/m<sup>2</sup>) are seen at a forward bias applied voltage of 3.37 V in the respectively simulated devices with the effect of the variation in thickness  $x=500^\circ\text{A}$  of the Exciton/Electron blocking layer as BCP and provided the highest blue light flow. Here Proposed OLED device has given the most increased illumination flux at a given voltage of 3.37 V with the highest J of 1.227819e5 (mA/cm<sup>2</sup>) of PMMA: Bepq2 polymer layer can entirely cover the blue area and validated through the Referenced results which show in Table 2.

The analysis of comparison results between proposed OLED device when variation of BCP layer is ( $x=50$  nm, 60 nm, 90 nm, 120 nm) with referenced device structure are presented in Table 2

**Table 2.** The analysis of comparison results between proposed OLED device when variation of BCP layer is ( $x=50$  nm, 60 nm, 90 nm, 120 nm) with referenced device structure

S.N.	OLED device /Parameters	Max. illumination flux (lumens/m <sup>2</sup> )	Threshold Voltage (V)	Max. EL ( $\lambda_{\text{max}}$ ) nm	Max. Current Efficiency (cd/A)	CIE coordinates
1.	Proposed Device BCP $x=50$ nm	1071956.76	3.37	450	87.3	(0.140, 0.140)
2.	Proposed Device BCP $x=50$ nm	829052.94	3.375	452	67.18	(0.142, 0.142)
3.	Proposed Device BCP $x=50$ nm	724655.26	3.38	455	58.7	(0.142, 0.142)
4.	Proposed Device BCP $x=50$ nm	636053.3	3.95	465	51.6	(0.15, 0.15)
5.	Ref. Device [21]	10611	4.1	530	20.1	(0.15, 0.15)

According to the simulation results shown in Figures 4, 5, and 6, current density rises if the thickness of PMMA is kept at a minimum. Due to the PEDOT: PSS layer's reduction in the hole barrier, due to the minimum thickness of the BCP layer as exciton/electron blocking layer used to the proposed OLED device has the highest current density of 1.127819e5 (mA/cm<sup>2</sup>) and most increased illumination flux of 1071956.76 (lumens/m<sup>2</sup>) and comparatively high light conversion efficiency with ref. device [21].

## CONCLUSION

We have reported the successful investigation of electrical and optical parameters (Max. Illumination flux, Max. CE, and current density of the novel multi-layered OLED device structure with a focus on the role of conductive layers (charge injection, transport, and emission layers) which used conductive materials (Spiro-MeOTAD, PMMA: Bepq2, BCP, Tpb, and LiF) have been

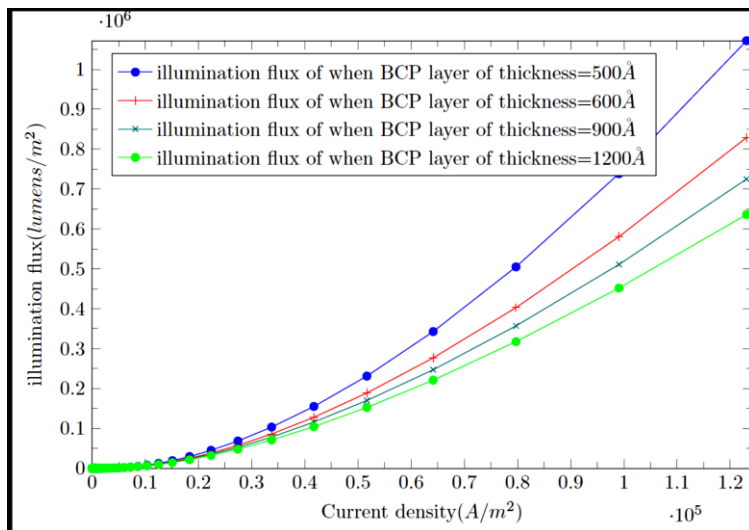


**Figure 4.** Illumination Flux ( $\text{lumens}/\text{m}^2$ ) v/s Current density ( $\text{mA}/\text{cm}^2$ ).

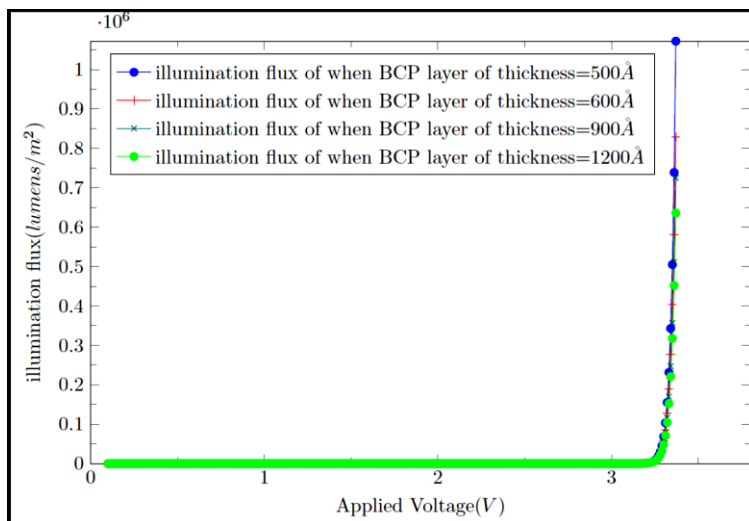


**Figure 5.** Illumination Flux ( $\text{lumens}/\text{m}^2$ ) v/s forward bias applied voltage (V).

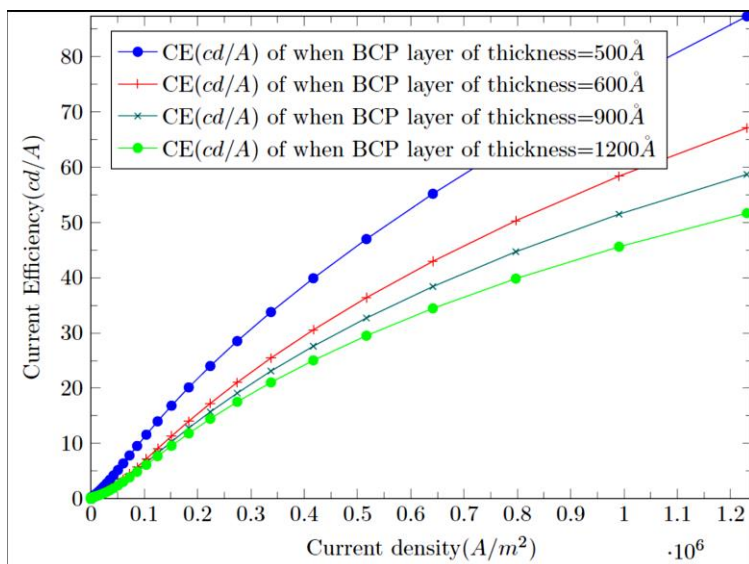


**Figure 6.** Current Efficiency ( $\text{cd}/\text{A}$ ) v/s Current density ( $\text{A}/\text{m}^2$ ).

sandwiched between (ITO) as the p-type electrode and Al as an n-type electrode. And we found Max. CE is 87.5(cd/A) with Max. Illumination flux is 1071956.76 (lumens/m<sup>2</sup>) seen at a minimum threshold voltage is 3.37 V when kept thickness of the BCP is minimum  $x=500^{\circ}\text{A}$  and provided the highest blue light flow. We have here the Proposed OLED device given the highest illumination flux at a given voltage of 3.37 V with the highest current density is 1.227819e5 (mA/cm<sup>2</sup>) with the CIE parameters remaining stable at (0.140,0.140) of PMMA: Bepq2 polymer layer can entirely cover nearest the blue area and validated through the Referenced results which show in Table 2 and compared with the proposed device at 450 nm wavelength using emission material PMMA: Bepq2. The study aims to pave the way for future research into the electro-optic effects of highly efficient and high-brightness OLED technology.

### Declaration of Interest

Authors should reveal any possible conflict of interest in their submitted manuscripts. A competing interest exists when professional judgment concerning the validity of work is influenced by a secondary interest, such as financial gain. The author(s) declare(s) that there is no conflict of interest regarding the publication of this manuscript.

### REFERENCES

1. M. Zhu and C. Yang, "Blue fluorescent emitters: design tactics and applications in organic light-emitting diodes," *Chemical Society Reviews*, vol. 42, no. 12, pp. 4963–4976, 2013.
2. S. O. Jeon, K. S. Yook, C. W. Joo, and J. Y. Lee, "High-efficiency deep blue-phosphorescent organic light-emitting diodes using a phosphine oxide and a phosphine sulfide high-triplet-energy host material with bipolar charge-transport properties," *Advanced Materials*, vol. 22, no. 16, pp. 1872–1876, 2010.
3. X. Liu, W. Liu, W. Dongyu, X. Wei, L. Wang, H. Wang, Y. Miao, H. Xu, J. Yu, and B. Xu, "Deep-blue fluorescent emitter based on a 9, 9-dioctylfluorene bridge with a hybridized local and charge-transfer excited state for organic light-emitting devices with EQE exceeding 8%," *Journal of Materials Chemistry C*, vol. 8, no. 40, pp. 14 117–14 124, 2020.
4. C. Si, Z. Li, K. Guo, X. Lv, S. Pan, G. Chen, Y. Hao, and B. Wei, "Functional versatile bipolar 3, 3-dimethyl-9, 9-bianthracene derivatives as an efficient host and deep-blue emitter," *Dyes and Pigments*, vol. 148, pp. 329–340, 2018.
5. H. Shin, Y. H. Ha, H.-G. Kim, R. Kim, S.-K. Kwon, Y.-H. Kim, and J.-J. Kim, "Controlling horizontal dipole orientation and emission spectrum of ir complexes by chemical design of ancillary ligands for efficient deep-blue organic light-emitting diodes," *Advanced Materials*, vol. 31, no. 21, p. 1808102, 2019.
6. X. Li, J. Zhang, Z. Zhao, L. Wang, H. Yang, Q. Chang, N. Jiang, Z. Liu, Z. Bian, W. Liu et al., "Deep blue phosphorescent organic light-emitting diodes with ciey value of 0.11 and external quantum efficiency up to 22.5%," *Advanced Materials*, vol. 30, no. 12, p. 1705005, 2018.
7. C. Fu, S. Luo, Z. Li, X. Ai, Z. Pang, C. Li, K. Chen, L. Zhou, F. Li, Y. Huang et al., "Highly efficient deep-blue oleds based on hybridized local and charge-transfer emitters bearing pyrene as the structural unit," *Chemical Communications*, vol. 55, no. 44, pp. 6317–6320, 2019.
8. R. Chavez III, M. Cai, B. Tlach, D. L. Wheeler, R. Kaudal, A. Tsyrenova, A. L. Tomlinson, R. Shinar, J. Shinar, and M. Jeffries-EL, "Benzobisoxazole cruciforms: a tuneable, cross-conjugated platform for the generation of deep blue oled materials," *Journal of Materials Chemistry C*, vol. 4, no. 17, pp. 3765–3773, 2016.
9. X. Zhan, N. Sun, Z. Wu, J. Tu, L. Yuan, X. Tang, Y. Xie, Q. Peng, Y. Dong, Q. Li et al., "Polyphenylbenzene as a platform for deep blue oleds: aggregation enhanced emission and high external quantum efficiency of 3.98%," *Chemistry of Materials*, vol. 27, no. 5, pp. 1847– 1854, 2015.
10. S. Hu, Y. Tian, Y. Lin, W. Shi, Y. Pang, S. Pan, and B. Wei, "High efficiency and long lifetime deep-blue organic light-emitting diode with a maximum external quantum efficiency of 20.6% and ciey of 0.04," *Dyes and Pigments*, vol. 205, p. 110548, 2022.

11. C.-Y. Chan, M. Tanaka, Y.-T. Lee, Y.-W. Wong, H. Nakanotani, T. Hatakeyama, and C. Adachi, "Stable pure-blue hyper fluorescence organic light-emitting diodes with high-efficiency and narrow emission," *Nature Photonics*, vol. 15, no. 3, pp. 203–207, 2021.
12. N. A. Kukhta and M. R. Bryce, "Dual emission in purely organic materials for optoelectronic applications," *Materials Horizons*, vol. 8, no. 1, pp. 33–55, 2021.
13. W. A. Ayalew and D. W. Ayele, "Dye-sensitized solar cells using natural dye as light-harvesting materials extracted from *acanthus sennii* chiovenda flower and *euphorbia cotinifolia* leaf," *Journal of science: Advanced materials and devices*, vol. 1, no. 4, pp. 488–494, 2016.
14. G. Sharma, A. Quraishi, S. Kattayat, S. Josey, S. Hashmi, M. Ezzeldien, S. L. Tripathi, P. Alvi et al., "Structure optimization and investigation of electrical and optical characteristics of alq3/taz: Ir (ppy) 3-bcp/hmtpd oled," *Optical and Quantum Electronics*, vol. 54, no. 5, pp. 1–13, 2022.
15. U. Ali, "Karim kj bt. a., buang na," A review of the properties and applications of poly (methyl methacrylate)(PMMA). *Polymer Rev*, vol. 55, pp. 678–705, 2015.
16. J. A. Röhler, *On Diffusion-Barriers in Space-Charge-Limited Current Measurements of Polymer Single-Carrier Devices*. Nanoscience, Niels Bohr Institute, Copenhagen University, 2013.
17. C.-C. Lee, Y.-D. Jong, P.-T. Huang, Y. C. Chen, P.-J. Hu, and Y. Chang, "Numerical simulation of electrical model for organic light-emitting devices with fluorescent dopant in the emitting layer," *Japanese journal of applied physics*, vol. 44, no. 11R, p. 8147, 2005.
18. C.-C. Lee, M.-Y. Chang, P.-T. Huang, Y. C. Chen, Y. Chang, and S.-W. Liu, "Electrical and optical simulation of organic light-emitting devices with fluorescent dopant in the emitting layer," *Journal of applied physics*, vol. 101, no. 11, p. 114501, 2007.
19. M. Pope, C. E. Swenberg et al., *Electronic processes in organic crystals and polymers*. Oxford University Press on Demand, 1999, vol. 56.
20. B. Sim, C.-K. Moon, K.-H. Kim, and J.-J. Kim, "Quantitative analysis of the efficiency of oleds," *ACS Applied Materials & Interfaces*, vol. 8, no. 48, pp. 33 010–33 018, 2016.
21. X. Zhang, J. Xie, Y. Zhang, R. Sun, S. Liu, W. Zhang, X. Zhang, and F. Hu, "Pmma doped composite films microlens arrays on a flexible substrate for improving extraction of an organic light-emitting diode," *Applied Optics*, vol. 61, no. 4, pp. 868–874, 2022.